Gerber et al., http://www.jcb.org/cgi/content/full/jcb.201409082/DC1

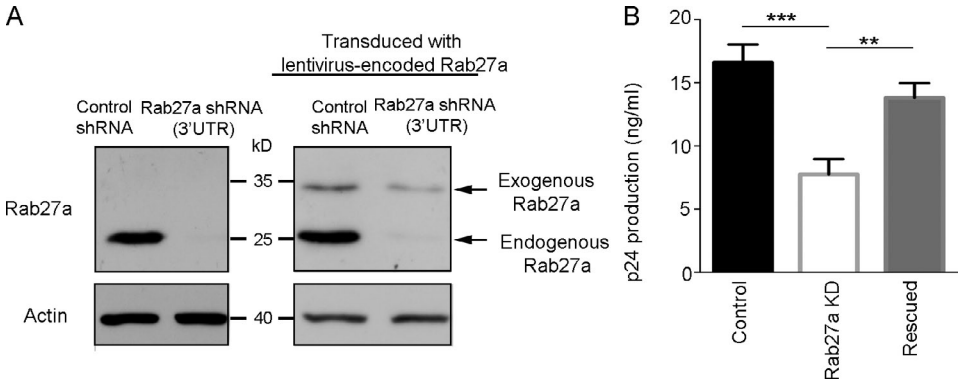

Figure S1. **Restoring Rab27a expression in cells expressing a Rab27a-shRNA reverts the inhibition of HIV-1 production observed in Rab27a-silenced cells.** Jurkat cells were transduced with a lentiviral vector encoding exogenous Rab27a fused to a 2A peptide sequence from *T. asigna* virus followed by GFP. Thus, Rab27a-expressing cells could be identified by the expression of GFP and isolated by FACS sorting. Sorted cells were subsequently transduced with either a control shRNA or a Rab27a shRNA targeting the 3′UTR of Rab27a gene. This strategy allowed us to silence the expression of endogenous Rab27a but not of the lentivirus-encoded Rab27a (exogenous). (A) Immunoblot analysis of Jurkat cells that express or do not express the exogenous Rab27a, which were subsequently treated with either a control shRNA or a Rab27a-3′UTR shRNA. Observe that the 3′UTR shRNA silences the expression of endogenous, but not exogenous, Rab27a. (B) Cells were infected with a VSV-G–pseudotyped HIV (20 ng p24/ml), and HIV-1 production was analyzed by quantifying the amount of p24 in cell culture supernatants at day 5 p.i. KD, knockdown. Error bars show SDs. **, $P < 0.01$; ***, $P < 0.001$.

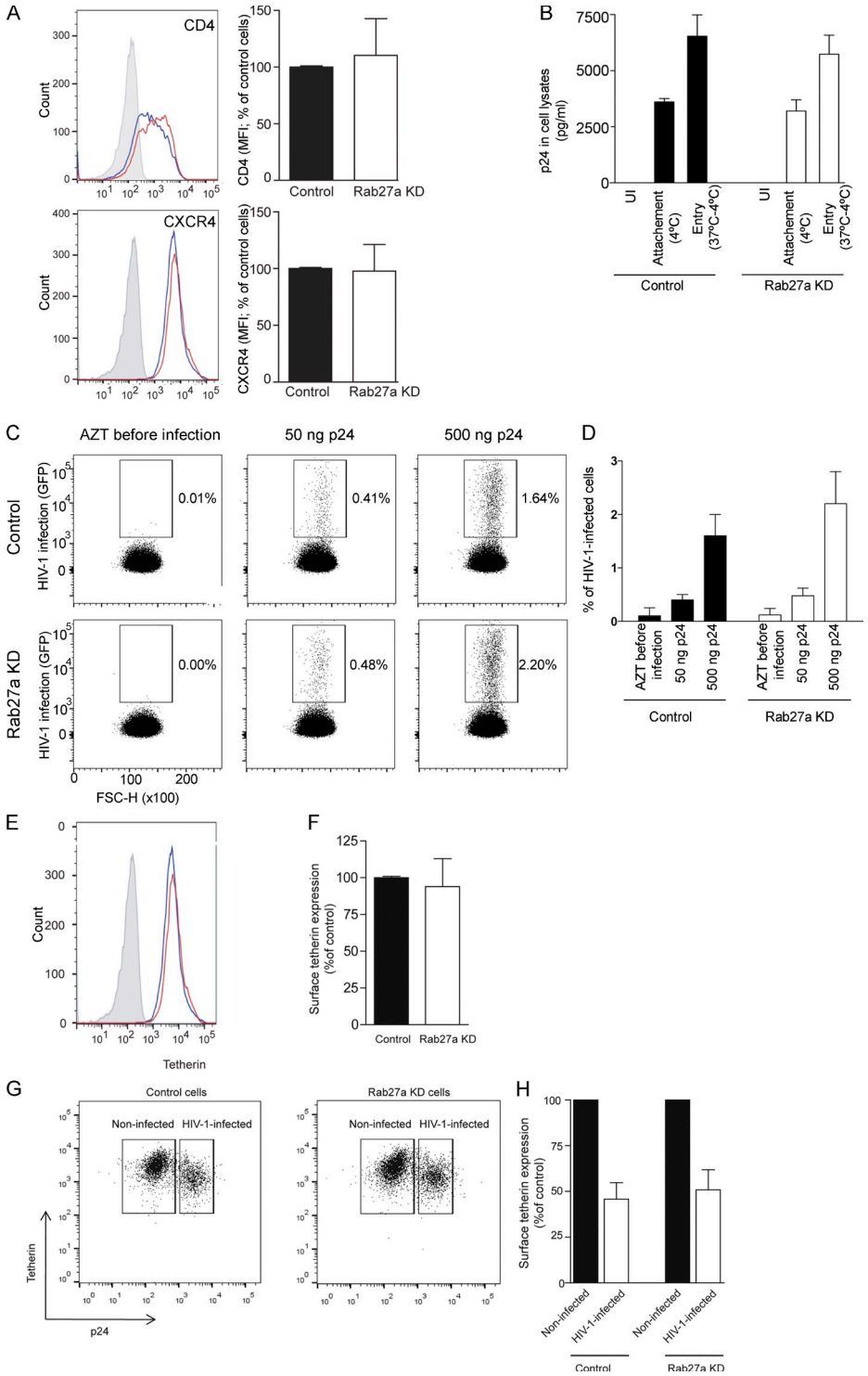

Figure S2. **The inhibition of HIV-1 replication observed in Rab27a-silenced cells is neither caused by a defect in viral entry nor in cell surface levels of tetherin.** (A) Cell surface expression levels of HIV-1 receptor CD4 (top) and coreceptor CXCR4 (bottom) were assessed by FACS analysis in control (blue lines) and Rab27a-silenced (red lines) cells. Isotype control is shown in gray. A histogram from a representative experiment and the means ± SD of three independent experiments are shown. MFI, mean fluorescence intensity. (B) HIV-1 attachment and entry were determined by incubating the cells with 50 ng/ml HIV-1 at 4°C or 37°C, respectively, for 90 min. After extensive washing, cells were lysed, and the amount of p24 in cell lysates was determined by ELISA. Entry was calculated as the difference in the values obtained at 37°C and at 4°C. Uninfected cells (UI) were added as negative control. Data from a representative experiment out of three performed in triplicates are shown. (C and D) The susceptibility of Rab27a-silenced cells to HIV-1 infection was assessed using a single cycle replication assay. Control and Rab27a-silenced Jurkat cells were infected with HIV-1 (50 or 500 ng p24) for 6 h at 37°C. Then, cells were washed to eliminate virus, and AZT was added to the culture medium to prevent secondary replication cycles. At 48 h after infection, the percentage of HIV-1–infected cells was assessed by FACS analysis. The efficiency of AZT to inhibit secondary replication was revealed by the lack of HIV-1–infected cells when AZT was added before infection. Dot plots (C) and the means ± SD of triplicate measurements from a representative experiment (D) are shown. In C, boxes represent the gate of HIV-1 infected cells, and the percentages of cells in these gates are indicated. (E–H) To rule out an effect of Rab27a on tetherin expression levels, cell surface expression of this restriction factor was evaluated by FACS analysis. Cell surface staining for endogenous tetherin was analyzed in control (blue line) and Rab27a-silenced (red line) uninfected Jurkat T cells. A representative histogram (E) and the means ± SD two experiments (F) are shown as percentages of control cells. IgG isotype control is shown in gray. Tetherin expression was also evaluated in Jurkat cells infected with VSV-G–pseudotyped NL4-3-IRES-EGFP. At 48 h p.i., cells were stained for cell surface tetherin and analyzed by FACS. A representative dot plot (G) and the means ± SD two experiments (H) are shown. Observe that the down-regulation of tetherin on the surface of GFP-positive (HIV-1 infected) Rab27a-silenced cells was comparable to that observed in control cells. Error bars show SDs. KD, knockdown.

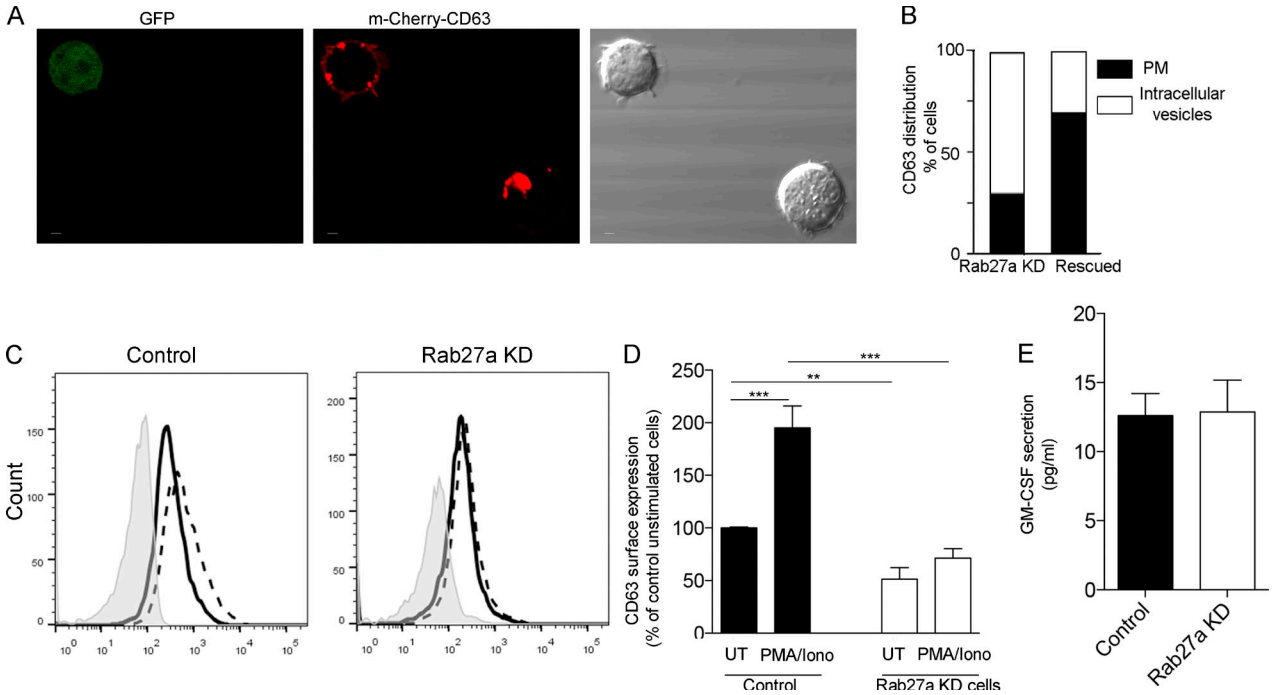

Figure S3. **Decreased CD63 cell surface expression in Rab27a-silenced cells.** (A) Restoring Rab27a expression in Jurkat cells expressing the 3′UTR Rab27a shRNA rescues the expression of CD63 at the PM. Shown are representative images of mCherry-CD63 distribution in Rab27a-silenced cells that were transduced (green cell) or not transduced with the Rab27a-encoding lentivirus. Bars, 2 µm. (B) Quantification was performed by blinded observers on a per-cell basis, in ≥50 cells of each condition. Data are expressed as percentages of cells in each category. (C and D) Induction of cell surface CD63 translocation. Control and Rab27a-silenced $CD4^+$ T cells were either untreated (UT) or stimulated with PMA-ionomycin (PMA/Iono) for 20 min in the presence of monensin and either FITC-labeled anti-CD63 Mab or isotype control. Cells were then washed and analyzed by FACS. (C) FACS plots showing CD63 expression in untreated (black solid lines) and PMA/Iono-stimulated cells (dashed lines). Isotype control is shown in gray. The data shown are from a single representative experiment out of three repeats. For the experiment shown, 10,000 cells from each condition were analyzed. (D) Graphs show the mean fluorescence intensity ± SD of CD63 staining. Results from a representative experiment of three performed with three independent healthy donors are shown. Data are expressed as percentages of control cells. (E) Cells (5×10^5/ml) were cultured for 18 h, and the secretion of GM-CSF was assessed by ELISA in cell culture supernatants. Error bars show SDs. KD, knockdown. **, $P < 0.01$.

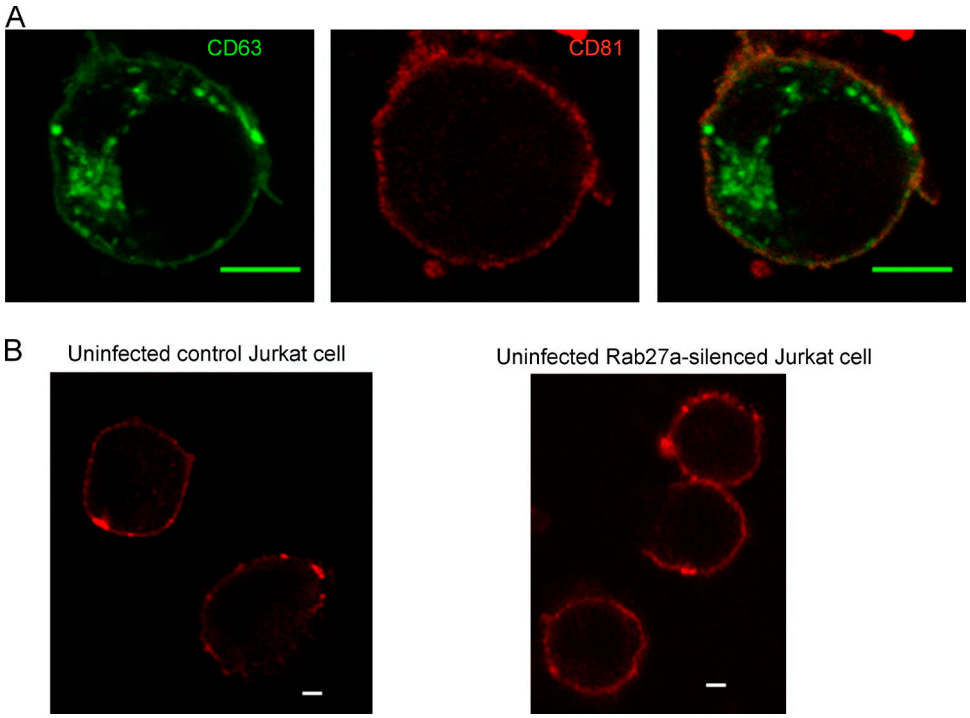

Figure S4. **Distribution of CD63 and CD81 in Jurkat cells.** (A) Representative LSCM image showing the distribution of CD63 and CD81 in control Jurkat cells. (B) Distribution of CD81 in control and Rab27a-silenced cells. Bars, 2 µm.

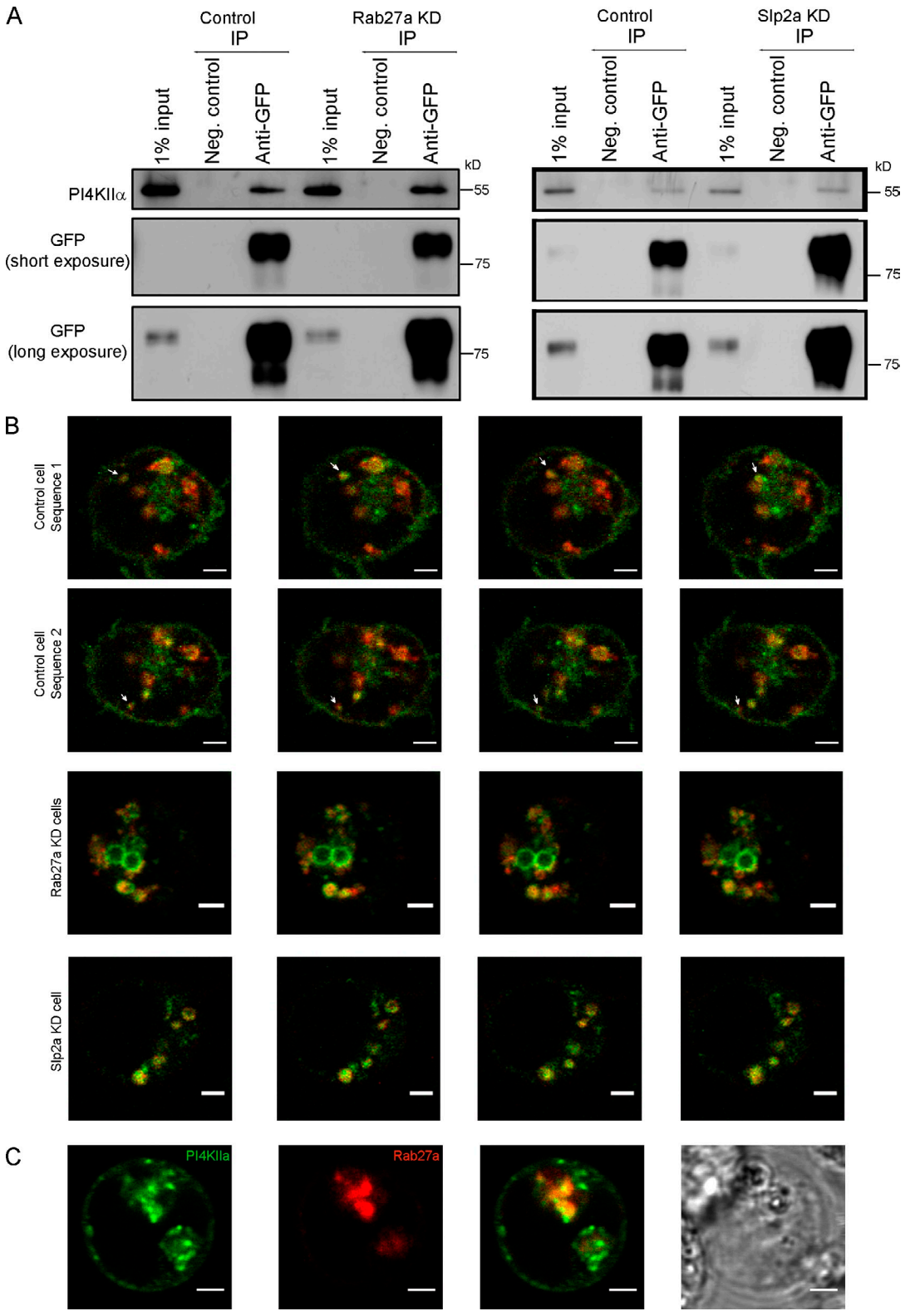

Figure S5. **PI4KIIα is associated with CD63/Rab27a-positive endosomes in Jurkat cells.** (A) The interaction between endogenous PI4KIIα and CD63-GFP in control, Rab27a-silenced and Slp2a-silenced cells was analyzed through GFP-trap precipitations from stably GFP-CD63–transfected Jurkat cells. Negative control corresponds to blocked beads. Efficiency of immune precipitation (IP) was assessed by detection of GFP in the cell lysate and precipitated material. A representative experiment of three is shown. (B) Selected sequential frames of time-lapse confocal microscopy of live control, Rab27a-silenced, and Slp2a-silenced Jurkat cells transfected to express both mCherry-CD63 (red) and GFP-PI4KIIα (green). Time between frames: 1.325 s (control cells) and 2.65 s (knockdown [KD] cells). Bars, 2 µm. Arrows in control cells show two vesicles with directional movement. (C) LSCM images of live Jurkat cells transfected to express dsRed-Rab27a and GFP-PI4KIIa. Transmission light channel is shown on the right. Bars, 2 µm.

Table S1. **qPCR analysis of the expression of Rab27 effector proteins in Jurkat cells**

Official symbol	Official name	Name also known as	Δ Ct in Jurkat cells[a]	Expression in Jurkat cells
SYTL1	Synaptotagmin-like 1	Slp1	10.1	Yes
SYTL2	Synaptotagmin-like 2	Slp2	7.8	Yes
SYTL3	Synaptotagmin-like 3	Slp3	8.3	Yes
SYTL4	Synaptotagmin-like 4	Slp4	0.0	No
EXPH5	Exophilin 5	Slac2b	12.4	Yes
MYRIP	Myosin VIIA and rab interacting protein	Slac2c	0.0	No
RPH3AL	Rabphilin 3A-like (without C2 domains)	Noc2	13.6	Yes
UNC13D	unc-13 homolog D	Munc13-4	12.2	Yes
TBC1D10B	TBC1 domain family member 10A	EPI64	13.0	Yes

[a]Δ Ct was calculated as the difference between the Ct obtained by qPCR using primers specific for the indicated gene, minus the Ct obtained in the same conditions in samples in which no reverse transcriptase was used for the reverse transcription reaction.

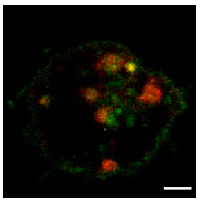

Video 1. **Localization and dynamics of mCherry-CD63 and GFP-PI4KIIα in control Jurkat cells.** Time-lapse confocal microscopy of live control Jurkat cells expressing both mCherry-CD63 (red) and GFP-PI4KIIα (green). Images were acquired using a laser-scanning confocal microscope (spectral FV 1000; Olympus). Frames were taken every 1.325 s for 2.5 min. The video plays at 6 frames per s (fps). Bar, 2 µm. Selected frames from this video are shown in Fig. S5 B. Arrows point to double-positive vesicles with long-range movements.

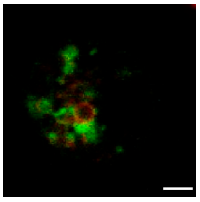

Video 2. **Localization and dynamics of mCherry-CD63 and GFP-PI4KIIα in Rab27a-silenced Jurkat cells.** Time-lapse confocal microscopy of live Rab27a-silenced Jurkat cells expressing both mCherry-CD63 (red) and GFP-PI4KIIα (green). Images were acquired using a laser-scanning confocal microscope (spectral FV 1000; Olympus). Frames were taken every 2.65 s for 3.7 min. The video plays at 3 fps. Bar, 2 µm. Selected frames from this video are shown in Fig. S5 B.

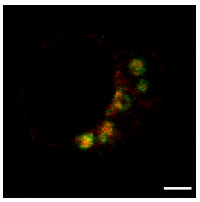

Video 3. **Localization and dynamics of mCherry-CD63 and GFP-PI4KIIα in Slp2a-silenced Jurkat cells.** Time-lapse confocal microscopy of live Slp2a-silenced Jurkat cells expressing both mCherry-CD63 (red) and GFP-PI4KIIα (green). Images were acquired using a laser-scanning confocal microscope (spectral FV 1000; Olympus). Frames were taken every 1.325 s for 2.5 min. The video plays at 6 fps. Bar, 2 µm. Selected frames from this video are shown in Fig. S5 B.